



A Journal of the Gesellschaft Deutscher Chemiker

Angewandte Chemie

GDCh

International Edition

www.angewandte.org

Accepted Article

Title: Electrochromic Poly(chalcogenoviologens) as Anode Materials for High-Performance Organic Radical Li-Ion Batteries

Authors: Guoping Li, Bingjie Zhang, Jianwei Wang, Hongyang Zhao, Wenqiang Ma, Letian Xu, Weidong Zhang, Kun Zhou, Yaping Du, and Gang He

This manuscript has been accepted after peer review and appears as an Accepted Article online prior to editing, proofing, and formal publication of the final Version of Record (VoR). This work is currently citable by using the Digital Object Identifier (DOI) given below. The VoR will be published online in Early View as soon as possible and may be different to this Accepted Article as a result of editing. Readers should obtain the VoR from the journal website shown below when it is published to ensure accuracy of information. The authors are responsible for the content of this Accepted Article.

To be cited as: *Angew. Chem. Int. Ed.* 10.1002/anie.201903152
Angew. Chem. 10.1002/ange.201903152

Link to VoR: <http://dx.doi.org/10.1002/anie.201903152>
<http://dx.doi.org/10.1002/ange.201903152>

COMMUNICATION

Electrochromic Poly(chalcogenoviologens) as Anode Materials for High-Performance Organic Radical Li-Ion Batteries

Guoping Li[†], Bingjie Zhang[†], Jianwei Wang, Hongyang Zhao, Wenqiang Ma, Letian Xu, Weidong Zhang, Kun Zhou, Yaping Du, and Gang He^{*}

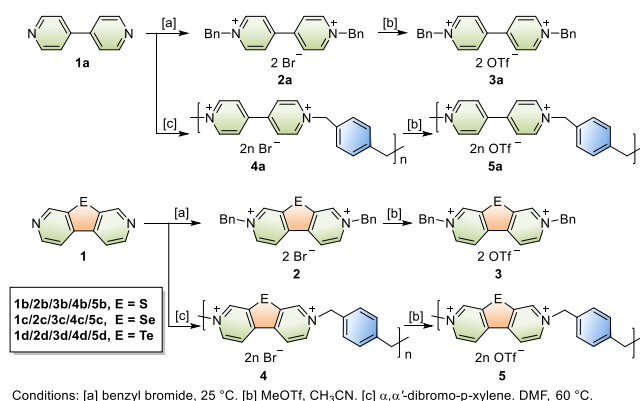
Abstract: A series of electrochromic electron-accepting poly(chalcogenoviologens) with multiple, stable and reversible redox centers are reported. They were used as anodic materials in organic radical Li-ion batteries (ORLIBs). Introduction of heavy atoms (S, Se, and Te) into viologen scaffold significantly improved the capacity and cycling stability of the ORLIBs. Notably, the poly(Te-BnV) anode had an intercalation ability of 20 Li-ions and showed higher conductivity and insolubility in the electrolyte, hence contributing to a reversible capacity of 502 mAh g⁻¹ at 100 mA g⁻¹ when the Coulombic efficiency approached 100%. To the best of our knowledge, the poly(Te-BnV) anode has the highest reported capacity to date for a viologen-based electrode. Based on their unique electrochromic and redox properties, flexible electrochromic batteries were fabricated, the charged/discharged state could be visually monitored. This work presents a promising avenue for the development of organic polymer-based electrodes for flexible hybrid visual electronics.

Viologens (RV²⁺) are electron-accepting organic molecules based on di-quaternized 4,4'-bipyridine moieties. Using applied voltage or direct illumination, viologens can undergo a two-step reversible one-electron reduction with obvious color changes. This phenomenon, commonly observed in the radical species of viologens (RV²⁺ + e⁻ ↔ RV^{•+}; RV^{•+} + e⁻ ↔ RV),^[1] has been explored in electrochromic devices (ECD),^[2] molecular machines,^[3] and organic batteries,^[4] and so on.^[5] Due to their synthetic versatility and easy tunability of redox properties,^[6] development of the viologen-based energy storage devices has increased dramatically over the past decades.^[7] The excellent redox properties and unique radical states of viologens make them exceptional electrode candidates for the new generation of energy storage devices, such as inorganic/organic Li/Na/Mg ion batteries,^[8] aqueous organic redox flow batteries,^[9] organic radical batteries,^[10] lithium-oxygen battery^[11] and so on.^[12] As one of the promising emerging technologies for energy storage,^[13] the ORBs have shown several advantages compared with the previously reported inorganic^[14] and polymeric materials,^[15] such as no need for rare metals, easy tunability of redox properties, more safety, and design flexibility at the molecular level, but the development of such batteries was still limited.^[16] The reported ORBs suffered from poor performance, e.g. low cell capacity and stabilities, due to fewer redox states and low specific energy.

Therefore, developing novel viologen derivatives with multiple stable redox centers and higher specific energy could dramatically enhance the performance and expand the limits of ORBs.^[8c]

The introduction of chalcogen atoms into organic conjugated scaffolds could enhance the compounds' electron mobility in terms of greater mass and polarizability.^[17] However, the inherent toxicity and shortage of the heavy chalcogenide resources may limit their applications, developing novel chalcogenide with low toxicity, low chalcogen content and high energy density via the modification of functional group is necessary to balance the toxicity and the shortage problems. Recently, our group developed thiocarboxylate compounds for organic sodium-ion battery electrodes and achieved high capacity and stability when four sulfur atoms were introduced, which demonstrated the benefit of atom substitution approach for organic batteries.^[18] In addition, we synthesized a series of novel chalcogenoviologens by introducing different chalcogen atoms (S, Se and Te), which achieved multicolor conversion in ECD and presented a combination of photosensitizer and electron mediator in visible-light-driven hydrogen evolution.^[19] The incorporation of chalcogen bridge resulted in rigid skeleton, stable radical states, extra redox centers and reduced HOMO–LUMO gap. With their multiple, stable redox properties, we have now focused on investigating chalcogenoviologens and their more insoluble polymeric moieties, poly(chalcogenoviologens) with low toxicity, low chalcogen content and high energy density as anodic materials in organic radical Li-ion batteries (ORLIBs).

To compare and contrast, benzylated viologens **2a/3a** and xylene-bridged polyviologens **4a/5a** were prepared. A series of related poly(chalcogenoviologens) **4b/4c/4d** were synthesized under similar benzylation reaction conditions (Scheme 1). Anion exchange in **4b/4c/4d** from bromide to triflate yielded dimethyl sulfoxide-D₆-soluble polymers **5b/5c/5d**. The ¹H upfield shift of α-pyridine occurred from 10.30 to 9.72 ppm with the introduction of



Scheme 1. Synthesis of poly(chalcogenoviologens).

[*] G. Li, B. Zhang, J. Wang, H. Zhao, Prof. Dr. G. He
Frontier Institute of Science and Technology, State Key Laboratory for Strength and Vibration of Mechanical Structures, Xi'an Key Laboratory of Sustainable Energy Materials Chemistry, Xi'an Jiaotong University, Xi'an, Shaanxi Province, 710054 (China)
E-mail: ganghe@mail.xjtu.edu.cn.

Prof. Dr. Y. Du

School of Materials Science and Engineering, National Institute for Advanced Materials, Nankai University, Tianjin, 300350 (China)

[*] These authors contributed equally to this work.

COMMUNICATION

heavier atoms due to p - π conjugation and increased electron density on the bipyridine skeleton. The NMR spectroscopy and mass spectrometry (Figures S35 and S36) showed that the polymers **4/5** had relatively low molecular weights, with ca. 12 repeat units. TGA analysis clarified that all benzylated viologen bromides were all stable under 200 °C (Figures S1–S3).

Compared to the corresponding viologen derivatives, poly(chalcogenoviologens) showed similar electron-accepting characteristics,^[8c] and their electrochemistry was probed via cyclic voltammetry (CV, Figure S4, and Table S1) with respect to Ag/AgCl/KCl reference electrode. There were two reversible one-electron reductions due to the presence of the bipyridine skeleton. Redox potentials of poly(chalcogenoviologens) were measured for **5b** ($E_{\text{red1},1/3} = -0.61$ V, $E_{\text{red2},1/3} = -1.04$ V, $E_{\text{red3},1/3} = -1.71$ V), **5c** ($E_{\text{red1},1/3} = -0.60$ V and $E_{\text{red2},1/3} = -0.95$ V, $E_{\text{red3},1/3} = -1.68$ V), and **5d** ($E_{\text{red1},1/3} = -0.58$ V and $E_{\text{red2},1/3} = -0.98$ V, $E_{\text{red3},1/3} = -1.66$ V). The semi-reversible reductive wave at -1.66 V in **5d** potentially arose from totally accepting electrons of polymer chains.^[8c] Due to the increase in electron density on the chalcogen atoms from poly(S-BnV) (**4b/5b**) to poly(Se-BnV) (**4c/5c**) to poly(Te-BnV) (**4d/5d**), the reductive wave from a chalcogenophene became increasingly pronounced, while a second semi-reversible reductive wave at -2.67 V in **2d** and **5d** originated from the introduction of Te atom. Heavy atom substitution in **5b/5c/5d** decreased their LUMO energy levels, therefore facilitating the reduction reaction.

The UV-vis spectra of poly(chalcogenoviologens) were similar to the benzylated chalcogenoviologens and consistent with the first singlet excitation energy obtained by time-dependent DFT (TD-DFT) calculations (Figure S5, Table S1, and Figures S25–S34). The maximum absorptions of **5b/5c/5d** in DMF were 394/419/484 nm, respectively. This red shift was accompanied by a band gap narrowing from 3.01 (**5b**) to 2.79 (**5c**) to 2.33 eV (**5d**). This result was attributed to the raised HOMO levels due to the stronger electron-donating character of the chalcogen atoms and reduced aromaticity of chalcogenoviologen units.

Spectroelectrochemical behaviors of **5b/5c/5d** were verified via proof-of-concept ECD, where these molecules showed similar electrochromic phenomena (Figures S6, S7, and 1a).^[20] For **5d**, with the applied potential of -0.7 V, the color gradually changed to dark blue and the absorption in the visible region increased due to the formation of radical species. This process resembles the chemical reduction with Zn (Figure 1b). When the potential of -1.2 V was applied, the decreased absorption in the visible region was

observed due to the accumulation of neutral species (Figure 1c); this process corresponds to the chemical reduction with Na.

Chalcogenoviologens (**2a/2b/2c/2d**) and their polymers (**4a/4b/4c/4d**) were tested as electrode materials in ORLIBs, due to the notable redox and electrochromic characteristics. Their electrochemical performances were measured using coin cells with lithium metal as the counter electrode in a potential range of 0.001–3.0 V vs. Li/Li⁺.

The electric conductivity and solubility of the electrode materials are the fundamental factors determining the battery performance.^[21] The electric conductivity was increased with the introduction of the chalcogen atoms as we observed a progressive deepening of the color (Figures S8 and S9) and a reduced band gap in the molecular (**2a** to **2d**) as well as polymeric moieties (**4a** to **4d**). Meanwhile, DFT calculations and conductivity tests via four probes method also confirmed this conjecture (Figure S10). Notably, the electric conductivity of **2d** (Te-BnV) was up to 0.096 $\mu\text{S cm}^{-1}$, which was 10 times higher than **2a/2b/2c**. As a member of the chalcogen family, heavier Te atom has special properties compared to S and Se atoms in terms of greater mass and polarizability; these properties are expected to improve the electron mobilities. In terms of electrode solubility, we found that the electrodes barely dissolved in the electrolyte in the first two hours and slightly dissolved after 4 hours (Figure S11). Remarkably, the solubilities of polyviologen electrodes were greatly reduced and the electric conductivities increased significantly (Figure S10), especially in the case of poly(Te-BnV) anode (**4d**, 0.13 $\mu\text{S cm}^{-1}$). The latter was insoluble in the electrolyte even after 40 charge/discharge cycles (Figure S12).

The electrochemical performances of ORLIBs measured against Li/Li⁺ were characterized by cyclic voltammetry (CV). Molecular benzylated viologens (**2a/2b/2c/2d**) and polymers (**4a/4b/4c/4d**) had similar redox states (Figures 2a, S4, S13, and S14). The difference of CV in solution and coin cell was attributed to the different measurement method and electrolytes. The CV in different electrolyte and potential window showed that the redox states in coin cells were consistent with the CV in DMF solution using lithium hexafluorophosphate as supporting electrolyte (Figure S4b–S4d).^[8c,22] Notably, the peak height and peak area below 1.2 V became pronouncedly enhanced from **4a** to **4b** to **4c** to **4d**; this phenomenon occurred due to the introduction of chalcogen atoms and the increased number of free electron pairs of the chalcogen atoms. The latter resulted in extra lithiation processes occurring on the chalcogen atoms, in particular on tellurium. Kinetic calculations illustrated that the electrochemical reaction was commanded by the synergistic effects of capacitive processes and diffusion-limited redox reaction. Notably, in the case of poly(Te-BnV) (**4d**), a 75% fraction of the total charge came from capacity-type contribution, which signified high rate and long cycling performance of the organic battery. This result was exceptional compared to other analogues. Furthermore, with an increased scan rate, the anodic peaks shifted to a higher potential in contrast to cathodic peaks, attributing to the increased polarization in **4d** (Figure S14). The linear fits of natural logarithm (ln) of peak current and scan rate revealed that the slopes of anodic and cathodic peaks were close to 1.0, illustrating that the reaction kinetics of the system **4d** is mainly controlled by the capacitance (Figure S18).^[23] The discharge/charge profiles of the molecular viologens (**2a/2b/2c/2d**) were similar and there was a tiny flat of the first discharge at 1.0 V, which came from the third reduction state—lithiation of bipyridine skeleton (Figures 2b, 2c,

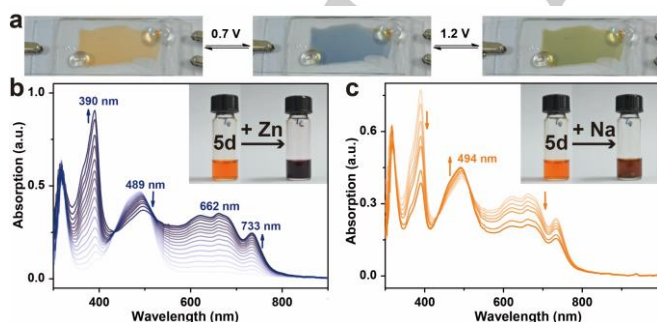


Figure 1. (a) Solution-based ECD with **5d**. (b) Spectroelectrochemistry of **5d** for first reduction and chemical reduction with Zn is shown as the inset. (c) Spectroelectrochemistry of **5d** for second reduction and chemical reduction with Na is shown as the inset.

COMMUNICATION

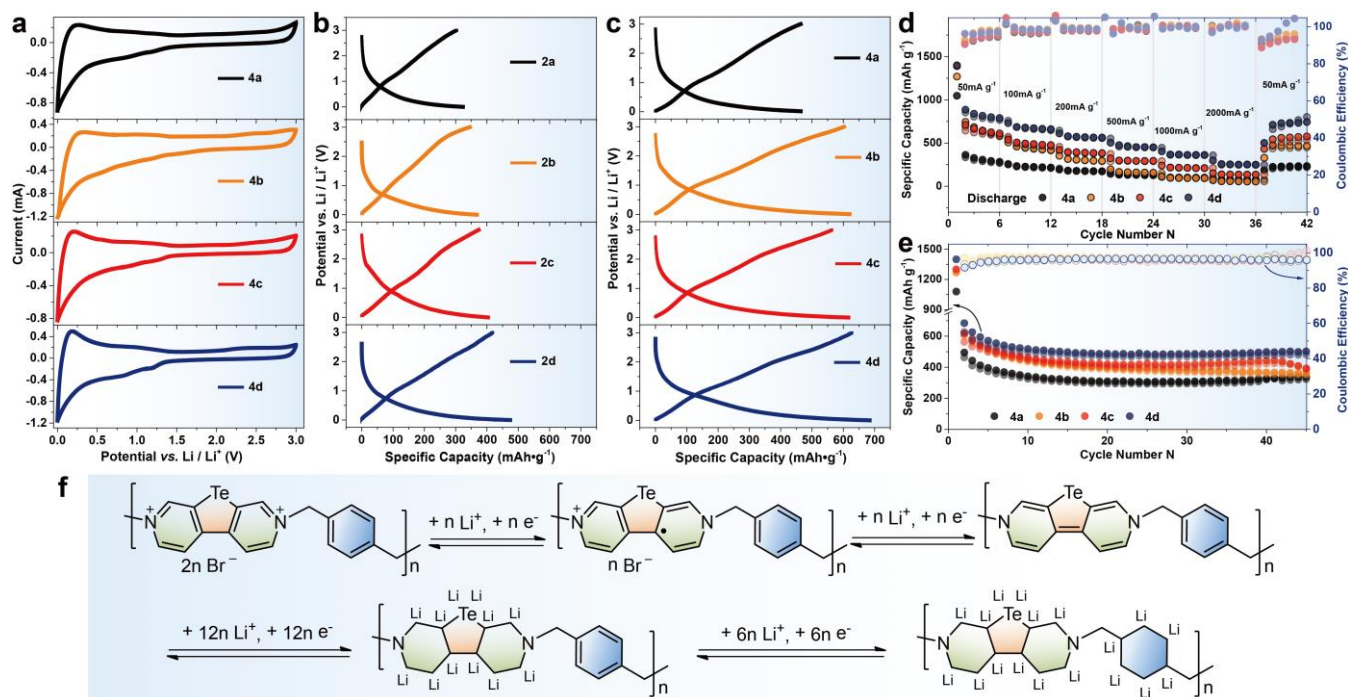


Figure 2. (a) The cyclic voltammograms at 0.5 mV s^{-1} of **4a-4d**. (b) Galvanostatic charge/discharge curves of **2a-2d** at 100 mA g^{-1} . (c) Galvanostatic charge/discharge curves of **4a-4d** at 100 mA g^{-1} . (d) Rate capability of **4a-4d**. (e) Cycle stability of **4a-4d** at 100 mA g^{-1} . (f) Schematic diagrams for the proposed electrochemical reduction steps of **4d**. (g) The first discharge potential profile of **4d** at 100 mA g^{-1} which correspond to the insertion of 1, 2, 4, 8, 14 and 20 Li-ions. The corresponding contribution by acetylene black was subtracted from all data.

S15, and S16). The second discharge capacities were gradually elevated with the substitution of heavier atoms and consistent with the CV curves (*i.e.*, the second discharge capacities at a current density of 100 mA g^{-1} of **2a**: 368 mAh g^{-1} , **2b**: 368 mAh g^{-1} , **2c**: 426 mAh g^{-1} , **2d**: 474 mAh g^{-1}). The irreversible capacities of the first discharge were caused by the formation of solid electrolyte interphase (SEI) layer.^[24] The specific discharge capacity of **2d** reduced to 238 mAh g^{-1} when the Coulombic efficiency approached 100%. All data were obtained after subtracting the corresponding contribution by the carbon black and the electrolyte.

Comparing the specific capacity and rate performance, Te-BnV (**2d**) revealed superior properties to **2a-2c** (Figure S17). This observation is consistent with the earlier noted superior behavior of poly(Te-BnV) **4d**. Poly(chalcogenoviologens) (**4a/4b/4c/4d**) had similar discharge/charge profiles to the corresponding monomers (Figure 2a), *e.g.*, the maximum second discharge capacity of 684 mAh g^{-1} at a current density of 100 mA g^{-1} was achieved for **4d** (Figure 2c). This was also atypical that better battery performances were in accompaniment with introduction of heavier atoms (*i.e.*, performance gradually improved from S to Se to Te). As shown in Figure 2d, poly(Te-BnV) (**4d**) electrode exhibited reversible capacities of 799, 684, 567, 463, and 366 mAh g^{-1} at current densities of 50, 100, 200, 500 and 1000 mA g^{-1} , respectively. It is worth noting that there was a retained capacity of 252 mAh g^{-1} as the current density increased to 2000 mA g^{-1} . When the current density dropped to 50 mA g^{-1} , a reversible capacity (750 mAh g^{-1}) returned even after 38 cycles. The irreversible capacities of the first discharge and the low initial Coulombic efficiency were caused by the lithiation of electronic

additives (carbonaceous material) and the formation of solid electrolyte interphase (SEI) layer. The capacity decay of **4a-4d** in the initial 20 cycles was attributed to slow formation of a stable SEI layer, which caused the low Coulombic efficiency ($<100\%$).^[24] The initial Coulombic efficiency was improved to 97% via loading **4d** on single-walled carbon nanotubes (SWNT) in polymerization process instead of adding acetylene black (Figure S24).^[16d,25] The specific discharge capacity became stable and reached 502 mAh g^{-1} when the Coulombic efficiency approached 100% (Figure 2e). In terms of capacity and cycling stability, poly(chalcogenoviologens), particularly for poly(Te-BnV) anode, have moderate performances compared with inorganic and polymeric electrodes. The capacity is even higher than some inorganic electrodes, such as 3DGN/MOF-derived CuO composite^[26] and the stability is better than Mn_3O_4 @B,N co-doped graphitic nanotubes,^[27] and typical polymeric radical materials, poly(2,2,6,6-tetramethylpiperidin-4-yl methacrylate) (Table S3).^[16e] The calculations of reaction free energy (ΔG) for the first and second steps of lithium insertion in **4a/4b/4c/4d** were obtained by DFT method and showed that **4d** had significantly lower free energy than other viologen derivatives (Figure S21).^[28]

The electrochemical kinetics of poly(chalcogenoviologens) were investigated using electrochemical impedance spectroscopy (EIS) (Figure S19). The smaller semicircle from **4a** to **4d** (Figure S20b) implied that resistances of the SEI films and the charge transfer reactions gradually ceased. The more perpendicular line showed the capacity-type contribution increased from **4a** to **4d**, which was agreement with the CV calculation. The reduced contact and charge-transfer resistances and increased capacity-

COMMUNICATION

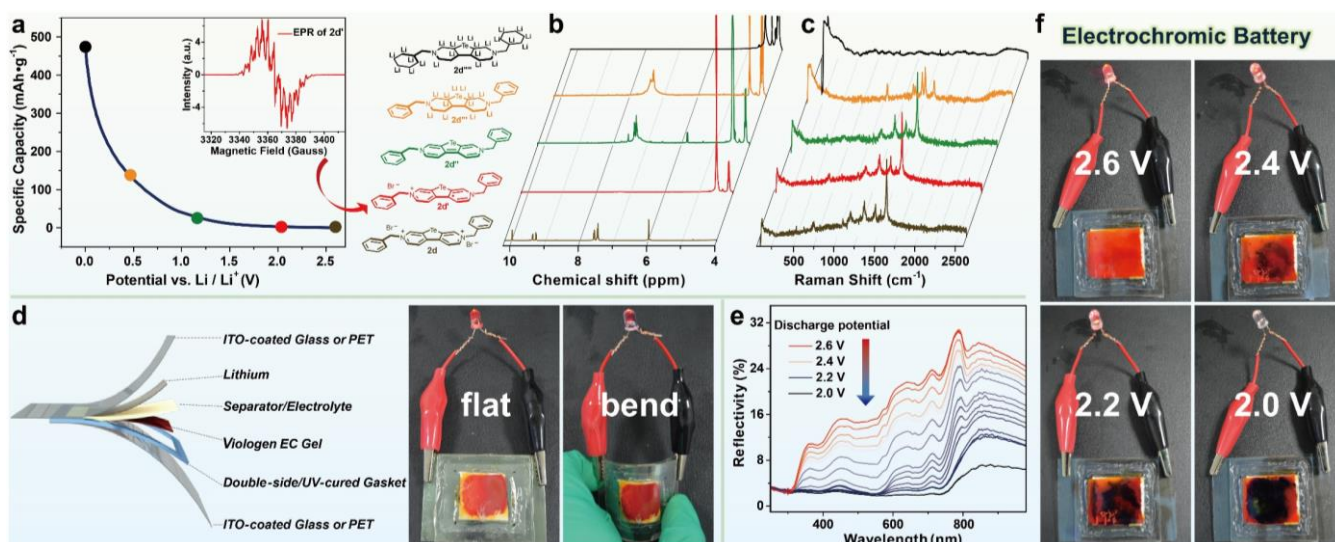


Figure 3. (a) The first discharge cycle of **2d**; EPR spectrum when the discharge potential decreased to 2.3 V is shown as an inset. (b) ^1H NMR and (c) *In situ* Raman spectroscopy for initial **2d** and after each of the four discharge potentials. (d) Device components of the fabricated flexible electrochromic battery. (e) *In situ* reflection spectroscopy and (f) Color changes in the process of discharge from 2.6 V to 2.3 V.

type contribution positively correlated with the better electric conductivity and higher capacity in heavier chalcogen-substituted analogues. The equivalent circuit was utilized to quantify the electrochemical kinetics (Figures S20c, and Table S2), the charge-transfer resistance (R_{ct}) decreased to 73.88 Ω for **4d**, electrochemical kinetics (Figures S20c, and Table S2), the charge-transfer resistance (R_{ct}) decreased to 73.88 Ω for **4d**, demonstrating faster charge-transfer kinetics and electric responses.^[29]

Calculations showed that one Li-ion insertion per unit of **4d** contributed to a theoretical capacity of 69.2 mAh g^{-1} and the lithiation process showed that each unit was capable of accepting 20 Li-ions;^[28] the initial two inserted Li-ions could be attributed to a reduction from **4d** to radical species **4d'** and reduction from **4d'** to neutral species **4d''**, respectively. Another two Li-ions could respectively insert into two sides of Te-bipyridine due to the semi-reversible reduction at -2.67 V (vs. Ag/AgCl) from Te atom and two electrons in the outer layers of Te in **4d**.^[30] The structure after lithiation of Te in **4d** was shown in Figure S22, which was verified by the DFT calculation, the ΔG indicated that the Li ion insertion of Te was a spontaneous reaction.^[31] The other 16 Li-ions could be inserted by the electrochemical reaction on the unsaturated carbons of the C5/C6 rings, as shown in Figures 2f.

The structure of the anode and their stability during battery operation are the determining factors of the device performance. To investigate the Li-ion intercalation effect, the structural changes between initial and discharged Te-BnV (**2d**, equivalent to a building block of polymer **4d**) was studied using ^1H NMR, electron paramagnetic resonance (EPR) and *in situ* Raman spectroscopies (Figures 3a–3c) due to insolubility of poly(chalcogenoviologens). The original **2d** exhibited a singlet and two multiplets in ^1H NMR with chemical shifts of 9.98 and 9.38 and 9.28 ppm, attributed to the bipyridine skeleton. When the discharge potential decreased to 2.1 V, the NMR signal completely disappeared due to the generation of radical species **2d'**, which were also confirmed by EPR spectroscopy (the inset

of Figure 3a). The upfield shift of ^1H resonances of the pyridine and unshifted ^1H resonances of the benzene ring were noted along with the decrease in discharge potential (to 1.2 V); this observation is in agreement with the formation of neutral species **2d''** (the green line in Figure 3b). When the discharge potential further decreased to 0.5 V, ^1H resonances of the pyridine nearly ceased, but ^1H resonances of the benzene ring persisted, *i.e.*, there were no more aromatic protons in the bipyridine skeleton due to the lithiation of viologen scaffold (**2d'''**, the orange line in Figure 3b). In addition, the new signal appeared in the upfield of ^1H NMR, corresponding to the completely lithiated molecule (**2d''''**, the black line in Figure 3b, to 0.001 V).^[32] The process of lithiation was also confirmed by *in situ* Raman spectroscopy (Figure 3c). The redox behavior and density functional theory (DFT) calculations, as well as the experimental study of structural changes of single building block (**2d**), commendably verified the predicted charge/discharge and lithiation mechanism of poly(chalcogenoviologens).

Unique electrochromic and redox properties of poly(chalcogenoviologens) allowed us to further develop the “smart” battery (in which the charged/discharged states are visible) and explore the field of flexible hybrid visual electronics.^[33] In this regard, a flexible electrochromic battery was fabricated using ITO-coated PET as a current collector and EC gel of **4d** as an electrode material (Figure 3d). In the process of discharge from 2.6 V to 2.0 V, the color of the electrochromic battery changed to purple and the reflectivity was significantly decreased on an entire wavelength scale (Figures 3e and 3f). We also tested the performance of a flexible cell using an aluminum film and a slurry coating method (Figure S23). This flexible cell showed good capacity and repeatability. Compared with inorganic or typical organic electrochromic batteries, such as $\text{KFe}^{\text{III}}[\text{Fe}^{\text{II}}(\text{CN})_6](\text{PB})$ ^[34] and WO_3 based batteries,^[35] the poly(chalcogenoviologens)-based batteries not only show higher capacity and cycle stability, but also possess better flexibility.

COMMUNICATION

In conclusion, a series of benzylated chalcogenoviologens and poly(chalcogenoviologens) with multiple, stable and reversible redox centers were synthesized. These molecules revealed excellent electron-accepting and electrochromic properties. Based on these novel characteristics, chalcogenoviologens and their polymers were tested as electrode materials in organic radical Li-ion batteries. With the introduction of heavier chalcogen atoms, the second discharge capacity and cycle stability were enhanced dramatically, especially in the case of Te-BnV (**2d**). Similarly, poly(chalcogenoviologens) showed promising high-performance rates and long-life cycles of ORLIBs. The maximum second discharge capacity of poly(Te-BnV) (**4d**) reached up to 684 mAh g⁻¹ at a current density of 100 mA g⁻¹ and the specific discharge capacity became stable and reached 502 mAh g⁻¹ when the Coulombic efficiency approached 100%, making it the highest reported capacity for a viologen-based electrode to date. This was attributed to the increased electric conductivity and extra lithiation processes on Te atom. These processes were examined in details and later applied in the fabrication of a flexible electrochromic battery. The explored versatile and efficient strategy offers a new platform for the development of next-generation high-capacity radical lithium-ion battery electrodes for flexible hybrid visual electronics.

Acknowledgements

This work was supported by the Natural Science Foundation of China (21704081, 21875180), the Fundamental Research Funds for the Central Universities (1191329805), Natural Science Foundation of Shaanxi province (2018JM2026), National 1000-Plan program, and the Cyrus Chung Ying Tang Foundation. We thank Drs. Yu Wang and Gang Chang and Axin Lu at Instrument Analysis Center of Xi'an Jiaotong University for their assistance with Raman spectroscopy and Elemental analysis and HRMS. We also thank Prof. Dingxin Liu for his help with EPR measurements.

Keywords: poly(chalcogenoviologens) • multiple redox centers • electrochromism • electrode materials • organic Li-ion batteries

- [1] L. A. Vermeulen, M. E. Thompson, *Nature* **1992**, *358*, 656-658.
- [2] a) A. N. Woodward, J. M. Kolesar, S. R. Hall, N.-A. Saleh, D. S. Jones, M. G. Walter, *J. Am. Chem. Soc.* **2017**, *139*, 8467-8473; b) H. Oh, D. G. Seo, T. Y. Yun, C. Y. Kim, H. C. Moon, *ACS Appl. Mater. Interfaces.* **2017**, *9*, 7658-7665.
- [3] a) Y. Li, Y. Dong, X. Miao, Y. Ren, B. Zhang, P. Wang, Y. Yu, B. Li, L. Isaacs, L. Cao, *Angew. Chem. Int. Ed.* **2018**, *130*, 737-741; b) M. C. Lipke, T. Cheng, Y. Wu, H. Arslan, H. Xiao, M. R. Wasielewski, W. A. Goddard, J. F. Stoddart, *J. Am. Chem. Soc.* **2017**, *139*, 3986-3998.
- [4] J. Luo, B. Hu, C. Debruler, T. L. Liu, *Angew. Chem. Int. Ed.* **2018**, *57*, 231-235.
- [5] a) Q. V. Nguyen, P. Martin, D. Frath, M. L. Della Rocca, F. Lafalet, S. Bellinck, P. Lafarge, J.-C. Lacroix, *J. Am. Chem. Soc.* **2018**, *140*, 10131-10134; b) C. Sun, G. Xu, X.-M. Jiang, G.-E. Wang, P.-Y. Guo, M.-S. Wang, G.-C. Guo, *J. Am. Chem. Soc.* **2018**, *140*, 2805-2811.
- [6] Y. Wu, J. Zhou, B. T. Phelan, C. M. Mauck, J. F. Stoddart, R. M. Young, M. R. Wasielewski, *J. Am. Chem. Soc.* **2017**, *139*, 14265-14276.
- [7] a) S. Sathyamoorthi, M. Kanagaraj, M. Kathiresan, V. Suryanarayanan, D. Velayutham, *J. Mater. Chem. A* **2016**, *4*, 4562-4569; b) L. Striepe, T. Baumgartner, *Chem. Eur. J.* **2017**, *23*, 16924-16940.
- [8] a) N. Kang, J. H. Park, J. Choi, J. Jin, J. Chun, I. G. Jung, J. Jeong, J.-G. Park, S. M. Lee, H. J. Kim, S. U. Son, *Angew. Chem. Int. Ed.* **2012**, *51*, 6626-6630; b) T. Gong, X. Lou, J.-J. Fang, E.-Q. Gao, B. Hu, *Dalton Trans.* **2016**, *45*, 19109-19116; c) M. Stolar, C. Reus, T. Baumgartner, *Adv. Energy Mater.* **2016**, *6*, 1600944; d) A. B. Ikhe, N. Naveen, K.-S. Sohn, M. Pyo, *Electrochim. Acta* **2018**, *283*, 393-400.
- [9] a) T. Janoschka, N. Martin, U. Martin, C. Friebe, S. Morgenstern, H. Hiller, M. D. Hager, U. S. Schubert, *Nature* **2015**, *527*, 78-81; b) T. Janoschka, N. Martin, M. D. Hager, U. S. Schubert, *Angew. Chem. Int. Ed.* **2016**, *55*, 14427-14430; c) T. Liu, X. Wei, Z. Nie, V. Sprenkle, W. Wang, *Adv. Energy Mater.* **2016**, *6*, 1501449-1501449; d) B. Hu, C. DeBruler, Z. Rhodes, T. L. Liu, *J. Am. Chem. Soc.* **2017**, *139*, 1207-1214; e) L. Fan, C. Jia, Y. G. Zhu, Q. Wang, *ACS Energy Lett.* **2017**, *2*, 615-621; f) C. DeBruler, B. Hu, J. Moss, X. Liu, J. Luo, Y. Sun, T. L. Liu, *Chem* **2017**, *3*, 961-978.
- [10] a) A. Ghosh, S. Mitra, *RSC Adv.* **2015**, *5*, 105632-105635; b) S. Sen, J. Saraidaridis, S. Y. Kim, G. T. R. Palmore, *ACS Appl. Mater. Interfaces.* **2013**, *5*, 7825-7830; c) S. M. Beladi-Mousavi, S. Sadaf, A. M. Mahmood, L. Walder, *ACS Nano* **2017**, *11*, 8730-8740.
- [11] a) M. J. Lacey, J. T. Frith, J. R. Owen, *Electrochem. Commun.* **2013**, *26*, 74-76; b) L. Yang, J. T. Frith, N. Garcia-Araez, J. R. Owen, *Chem. Commun.* **2015**, *51*, 1705-1708.
- [12] a) L. Cao, S. Sadaf, S. M. Beladi-Mousavi, L. Walder, *Eur. Polym. J.* **2013**, *49*, 1923-1934; b) N. Sano, W. Tomita, S. Hara, C.-M. Min, J.-S. Lee, K. Oyaizu, H. Nishide, *ACS Appl. Mater. Interfaces.* **2013**, *5*, 1355-1361; c) M. Yao, H. Sano, H. Ando, T. Kiyobayashi, *Sci. Rep.* **2015**, *5*, 10962; d) H. Wu, Y. Cao, L. Geng, C. Wang, *Chem. Mater.* **2017**, *29*, 3572-3579; e) S. Peticarari, Y. Sayed-Ahmad-Baraza, C. Ewels, P. Moreau, D. Guyomard, P. Poizat, F. Odobel, J. Gaubicher, *Adv. Energy Mater.* **2018**, *8*, 1701988.
- [13] a) Y. H. Zhu, Y. B. Yin, X. Yang, T. Sun, S. Wang, Y. S. Jiang, J. M. Yan, X. B. Zhang, *Angew. Chem. Int. Ed.* **2017**, *56*, 7881-7885; b) R. A. Rincón, G. Heydenrych, *Batteries & Supercaps* **2018**, *1*, 3-5; c) M. Duduta, S. de Rivaz, D. R. Clarke, R. J. Wood, *Batteries & Supercaps* **2018**, *1*, 131-134; d) N. Hergué, B. Ernould, A. Minoia, R. Lazzaroni, J.-F. Gohy, P. Dubois, O. Coulembier, *Batteries & Supercaps* **2018**, *1*, 102-109; e) R. Vaidya, V. Selvan, P. Badami, K. Knoop, A. M. Kannan, *Batteries & Supercaps* **2018**, *1*, 75-82; f) Y. H. Zhu, X. Yang, X. B. Zhang, *Angew. Chem. Int. Ed.* **2017**, *56*, 6378-6380.
- [14] a) M. Winter, B. Barnett, K. Xu, *Chem. Rev.* **2018**, *118*, 11433-11456; b) C. Chen, X. Xie, B. Anasori, A. Sarycheva, T. Makaryan, M. Zhao, P. Urbankowski, L. Miao, J. Jiang, Y. Gogotsi, *Angew. Chem. Int. Ed.* **2018**, *57*, 1846-1850; c) X. Chi, Y. Liang, F. Hao, Y. Zhang, J. Whiteley, H. Dong, P. Hu, S. Lee, Y. Yao, *Angew. Chem. Int. Ed.* **2018**, *57*, 2630-2634.
- [15] a) S. Muench, A. Wild, C. Friebe, B. Hauptler, T. Janoschka, U. S. Schubert, *Chem. Rev.* **2016**, *116*, 9438-9484; b) N. Wang, J. He, Z. Tu, Z. Yang, F. Zhao, X. Li, C. Huang, K. Wang, T. Jiu, Y. Yi, Y. Li, *Angew. Chem. Int. Ed.* **2017**, *56*, 10740-10745; c) Y. Zhang, J. Duan, D. Ma, P. Li, S. Li, H. Li, J. Zhou, X. Ma, X. Feng, B. Wang, *Angew. Chem. Int. Ed.* **2017**, *56*, 16313-16317.
- [16] a) L. Bugnon, C. J. H. Morton, P. Novak, J. Vetter, P. Nesvadba, *Chem. Mater.* **2007**, *19*, 2910-2914; b) Y. Imada, H. Nakano, K. Furukawa, R. Kishi, M. Nakano, H. Maruyama, M. Nakamoto, A. Sekiguchi, M. Ogawa, T. Ohta, Y. Yamamoto, *J. Am. Chem. Soc.* **2016**, *138*, 479-482; c) H. Tokue, T. Murata, H. Agatsuma, H. Nishide, K. Oyaizu, *Macromolecules* **2017**, *50*, 1950-1958; d) K. Hatakeyama-Sato, H. Wakamatsu, R. Katagiri, K. Oyaizu, H. Nishide, *Adv. Mater.* **2018**, *30*, 1800900; e) K. A. Hansen, J. Nerkar, K. Thomas, S. E. Bottle, A. P. O'Mullane, P. C. Talbot, J. P. Blinco, *ACS Appl. Mater. Interfaces.* **2018**, *10*, 7982-7988.
- [17] a) G. He, L. Kang, W. Torres Delgado, O. Shynkaruk, M. J. Ferguson, R. McDonald, E. Rivard, *J. Am. Chem. Soc.* **2013**, *135*, 5360-5363; b) G. He, W. Torres Delgado, D. J. Schatz, C. Merten, A. Mohammadpour, L. Mayr, M. J. Ferguson, R. McDonald, A. Brown, K. Shankar, E. Rivard, *Angew. Chem. Int. Ed.* **2014**, *53*, 4587-4591; c) A. J. Tilley, C. Guo, M. B. Miltenburg, T. B. Schon, H. Yan, Y. Li, D. S. Seferos, *Adv. Funct. Mater.* **2015**, *25*, 3321-3329; d) L. Xu, G. Li, T. Xu, W. Zhang, S. Zhang, S. Yin, Z. An, G. He, *Chem. Commun.* **2018**, *54*, 9226-9229.
- [18] H. Zhao, J. Wang, Y. Zheng, J. Li, X. Han, G. He, Y. Du, *Angew. Chem. Int. Ed.* **2017**, *56*, 15334-15338.
- [19] G. Li, L. Xu, W. Zhang, K. Zhou, Y. Ding, F. Liu, X. He, G. He, *Angew. Chem. Int. Ed.* **2018**, *57*, 4897-4901.
- [20] M. Stolar, J. Borau-Garcia, M. Toonen, T. Baumgartner, *J. Am. Chem. Soc.* **2015**, *137*, 3366-3371.
- [21] Q. Zhao, Z. Zhu, J. Chen, *Adv. Mater.* **2017**, *29*, 1607007.
- [22] J. Wu, X. Rui, G. Long, W. Chen, Q. Yan, Q. Zhang, *Angew. Chem. Int. Ed.* **2015**, *54*, 7354-7358.

COMMUNICATION

- [23] C. Luo, G. L. Xu, X. Ji, S. Hou, L. Chen, F. Wang, J. Jiang, Z. Chen, Y. Ren, K. Amine, C. Wang, *Angew. Chem. Int. Ed.* **2018**, *57*, 2879-2883.
- [24] a) T. Sun, Z.-J. Li, H.-G. Wang, D. Bao, F.-L. Meng, X.-B. Zhang, *Angew. Chem. Int. Ed.* **2016**, *55*, 10662-10666; b) K. A. See, M. A. Lumley, G. D. Stucky, C. P. Grey, R. Seshadri, *J. Electrochem. Soc.* **2017**, *164*, A327-A333; c) X. Fan, F. Wang, X. Ji, R. Wang, T. Gao, S. Hou, J. Chen, T. Deng, X. Li, L. Chen, C. Luo, L. Wang, C. Wang, *Angew. Chem. Int. Ed.* **2018**, *57*, 7146-7150.
- [25] H. Wu, Q. Meng, Q. Yang, M. Zhang, K. Lu, Z. Wei, *Adv. Mater.* **2015**, *27*, 6504-6510.
- [26] D. Ji, H. Zhou, Y. Tong, J. Wang, M. Zhu, T. Chen, A. Yuan, *Chem. Eng. J.* **2017**, *313*, 1623-1632.
- [27] H. Tabassum, R. Zou, A. Mahmood, Z. Liang, Q. Wang, H. Zhang, S. Gao, C. Qu, W. Guo, S. Guo, *Adv. Mater.* **2018**, *30*, 1705441.
- [28] S. Renault, V. A. Oltean, C. M. Araujo, A. Grigoriev, K. Edström, D. Brandell, *Chem. Mater.* **2016**, *28*, 1920-1926.
- [29] J. Wu, X. Rui, C. Wang, W.-B. Pei, R. Lau, Q. Yan, Q. Zhang, *Adv. Energy Mater.* **2015**, *5*, 1402189.
- [30] a) C. Han, Z. Li, W.-j. Li, S.-l. Chou, S.-x. Dou, *J. Mater. Chem. A* **2014**, *2*, 11683-11690; b) T. Koketsu, B. Paul, C. Wu, R. Kraehnert, Y. Huang, P. Strasser, *J. Appl. Electrochem.* **2016**, *46*, 627-633; c) A. R. Park, C. M. Park, *ACS Nano* **2017**, *11*, 6074-6084; d) X. Han, G. Qing, J. Sun, T. Sun, *Angew. Chem. Int. Ed.* **2012**, *51*, 5147-5151.
- [31] a) P.-T. Chen, F.-H. Yang, T. Sangeetha, H.-M. Gao, K. D. Huang, *Batteries & Supercaps* **2018**, *1*, 209-214; b) T. Sun, Z.-J. Li, X.-B. Zhang, *Research* **2018**, *2018*, 1-10.
- [32] D. C. Elias, R. R. Nair, T. M. G. Mohiuddin, S. V. Morozov, P. Blake, M. P. Halsall, A. C. Ferrari, D. W. Boukhvalov, M. I. Katsnelson, A. K. Geim, K. S. Novoselov, *Science* **2009**, *323*, 610-613.
- [33] Y. Guo, W. Li, H. Yu, D. F. Perepichka, H. Meng, *Adv. Energy Mater.* **2017**, *7*, 1601623.
- [34] J. Wang, L. Zhang, L. Yu, Z. Jiao, H. Xie, X. W. Lou, X. Sun, *Nat. Commun.* **2014**, *5*, 4921.
- [35] a) J. Zhao, Y. Tian, Z. Wang, S. Cong, D. Zhou, Q. Zhang, M. Yang, W. Zhang, F. Geng, Z. Zhao, *Angew. Chem. Int. Ed.* **2016**, *55*, 7161-7165; b) X. Xia, Z. Ku, D. Zhou, Y. Zhong, Y. Zhang, Y. Wang, M. J. Huang, J. Tu, H. J. Fan, *Mater. Horiz.* **2016**, *3*, 588-595.

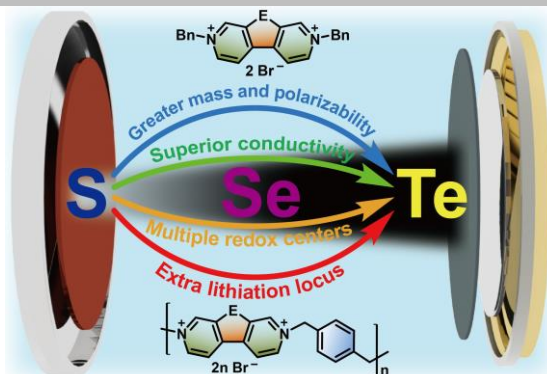
COMMUNICATION

Entry for the Table of Contents (Please choose one layout)

Layout 1:

COMMUNICATION

A new series of electrochromic poly(chalcogenoviologens) were used as anodes to fabricate “smart” high-performance organic radical Li-ion batteries. Introduction of the heavy atoms (S, Se, and Te) dramatically improved their capacity and cycling stability, leading to the discovery of the highest reported capacity to date for a viologen-based electrode.



Guoping Li[†], Bingjie Zhang[†],
Jianwei Wang, Hongyang Zhao,
Wenqiang Ma, Letian Xu, Weidong
Zhang, Kun Zhou, Yaping Du, and
Gang He*

Page No. – Page No.

**Electrochromic
Poly(chalcogenoviologens) as
Anode Materials for High
Performance Organic Radical Li-
ion Batteries**